Volume 13 | Number 45 | 7 December 2017 | Pages 8341–8662

Soft Matter

rsc.li/soft-matter-journal

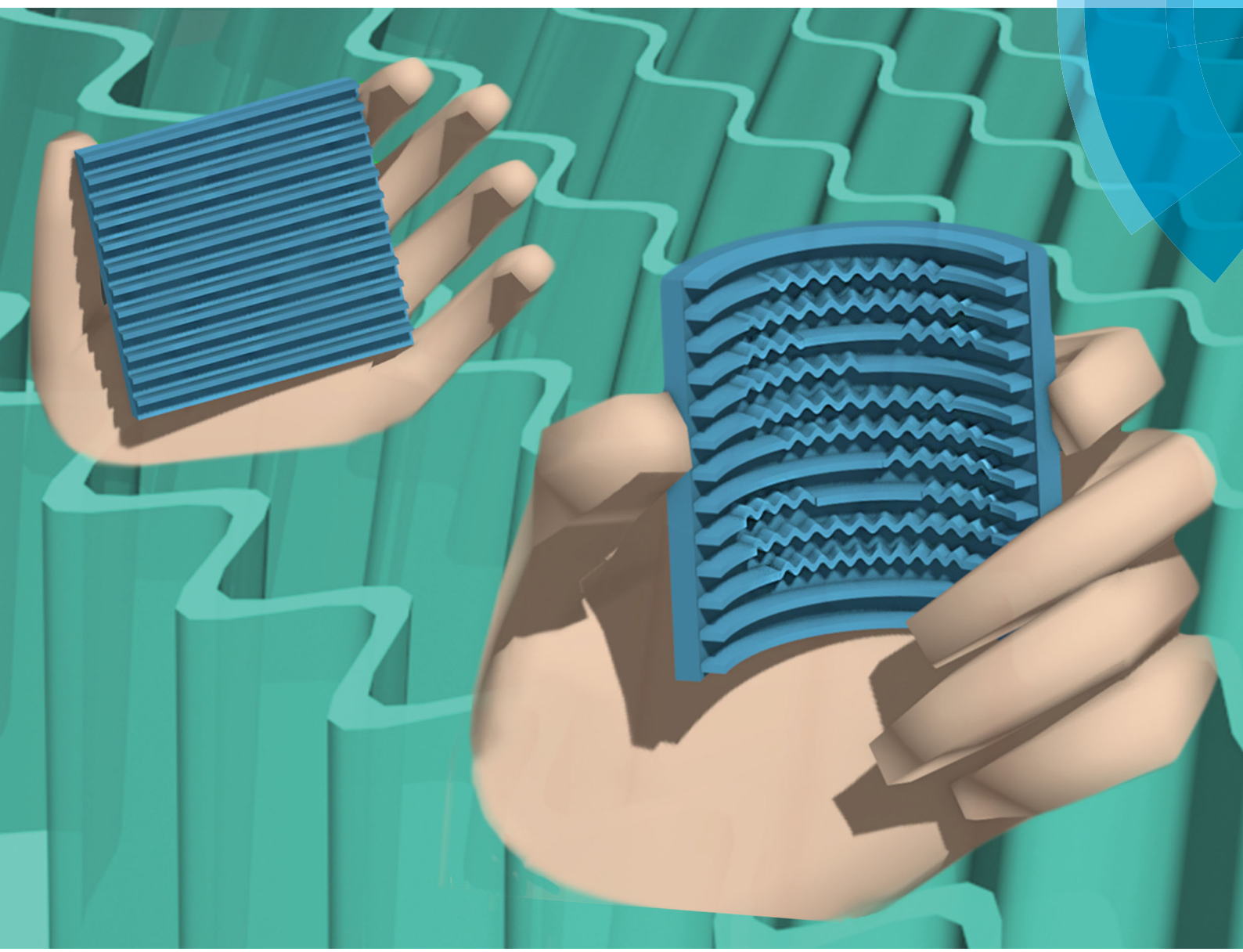

ISSN 1744-6848

ROYAL SOCIETY OF CHEMISTRY

COMMUNICATION

Won Bo Lee, Hyunsik Yoon *et al.*

Mechano-responsive lateral buckling of miniaturized beams standing on flexible substrates

Soft Matter

COMMUNICATION

View Article Online
View Journal | View Issue

Cite this: *Soft Matter*, 2017, **13**, 8357

Received 10th September 2017,
Accepted 29th October 2017

DOI: 10.1039/c7sm01822c

rsc.li/soft-matter-journal

Mechano-responsive lateral buckling of miniaturized beams standing on flexible substrates†

Hyemin Lee,[a] Jung Gun Bae,[b] Won Bo Lee *[b] and Hyunsik Yoon *[a]

We fabricate an elastomeric beam standing on a flexible substrate using 3D printing and soft lithography and investigate lateral buckling generated in the part of the wall when this beam is under pure bending. We also observe changes in the morphology of wrinkling along the applied strain and geometry of the wall, and then analyze it with scaling concepts. Furthermore, the degree of lateral buckling is controlled through the tip design in the ratchet structure and it is verified with finite element simulation. Based on this, a millimeter scale device with a visual difference according to the curvature is manufactured.

In mechanical or civil engineering, preventing large unwanted structural deformations such as buckling has been an important issue.[1,2] In particular, it is very important that deflections occur in bridges, railways or the skeletons of buildings. Nevertheless, it is almost impossible to create an environment in which deformation does not occur from various factors, such as external loading as well as heat-induced expansion or shrinkage. For this reason, in the field of structural mechanics, critical points have been studied where buckling begins to occur on the elements – *e.g.* slender, panel, *etc.* – of the structure.[1,3,4] Since the purpose of these studies was to prevent failure problems, the regime beyond the critical stress has received less attention. In the 1990s, however, research on the principle and method of buckling/wrinkling formation became active.[5–8] It was because of not only various types of wrinkles found in nature, but also the technological usefulness of micro- and nanoscale buckling.[9–12] Most of the studies were done on a bilayer system consisting of a thin hard skin which is subjected to compressive stress, bonded to a relatively thick soft substrate.[13–17] Therefore, research on the characteristic length of wrinkles, such as wavelength or amplitude, in a bilayer system is almost finished.[18–21] On the other hand, in recent years, research has begun on the transformation of a high aspect ratio freely standing wall to periodically undulated patterns. Specifically, methods for generating these wavy walls, such as thermal evaporation or swelling of polymers, have been introduced in the literature.[22,23] There was also a study on the change of instability mode in edge wrinkling due to compression according to the geometry of ridges.[24] Thus, it still remains intriguing to study the instability of this lateral buckling.

In this work, we present lateral buckling induced by bending of elastomeric wall structures attached on a flexible substrate. Here, we regard these structures as miniaturized beams, since the length of the lateral direction is long enough. Then inspired from the classical beam theory,[1,4,25] we control the configuration of the wrinkles. This simple yet research worthwhile system has several advantages compared with the previous work: (1) it is easy to create wrinkles without specific experimental equipment or complex processes, (2) the material can be deformed very rapidly as well as quasi-permanently in a reversible way and (3) the uncertainity from the poorly defined interface in the bilayer system – *e.g.* unclear or poor uniformity of materials – can be eliminated through the design of accurate dimensions (width and height of walls) and material properties (Young's modulus, Poisson's ratio, *etc.*), so it is suitable for a robust study on buckling because clear reverification of its basic mechanism is possible. Based on our experiment and theoretical analysis, we control the formation and morphology of lateral buckling. From this method, the mechanically responsive visual difference observed in our system is also investigated.

Fig. 1a conceptually shows lateral buckling caused by the pure bending of a line patterned elastomeric beam on the millimetre scale. It was fabricated with polydimethylsiloxane (PDMS) through soft lithography with a master prepared by a commercial 3D printer. The compressive strain is applied due to bending of the beam, and then confinement at the base of the wall leads to the transformation of straight line patterns into sinusoidal curves. When removing the given curvature, it instantaneously returns to the original state from the deformed state.

[a] *Department of Chemical and Biomolecular Engineering, Department of New Energy Engineering, Seoul National University of Science & Technology, Seoul, 01811, Korea. E-mail: hsyoon@seoultech.ac.kr*
[b] *School of Chemical and Biological Engineering, Institute of Chemical Processes, Seoul National University, Seoul, 08826, Korea. E-mail: wblee@snu.ac.kr*

† Electronic supplementary information (ESI) available. See DOI: 10.1039/c7sm01822c

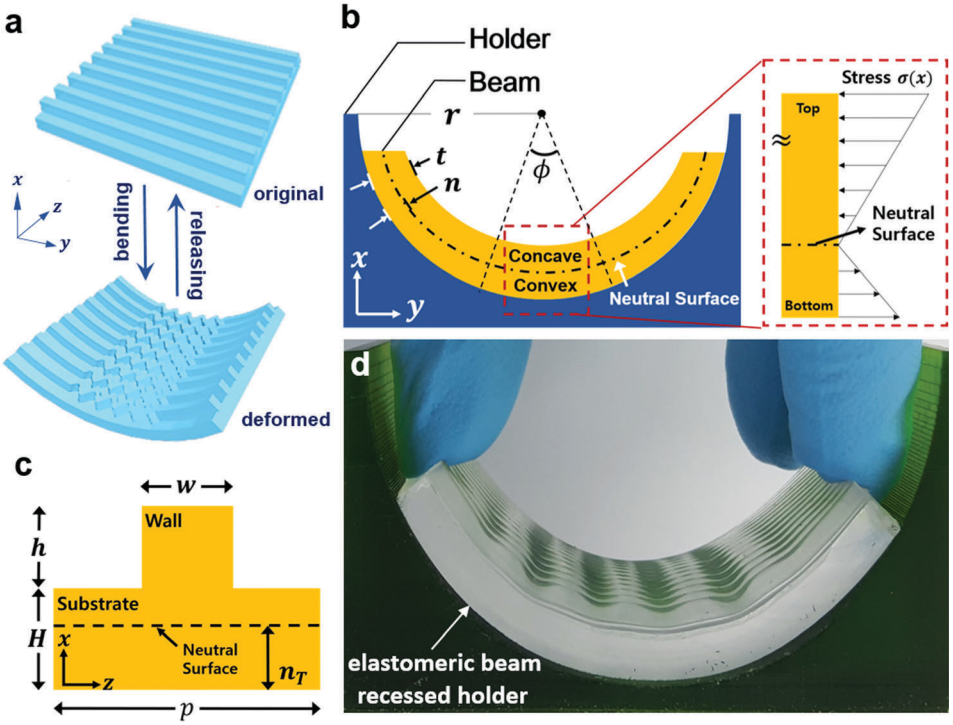

Fig. 1 (a) Conceptual illustration of lateral buckling formation with pure bending. (b) Schematic illustration of the elastomeric beam fixed in a recessed holder for bending and stress distribution at concave and convex parts of the beam divided by a neutral surface (Fig. S1, ESI†). (c) Schematic illustration of the T-shaped beam, which consists of wall and substrate parts. (d) Images of lateral buckling induced by bending.

To maintain a constant bending moment, the beam of thickness t is fixed in a recessed holder of radius r (Fig. 1b). When the beam is bent, it is divided into concave and convex parts. Between both of them, there is a surface named the neutral surface that does not undergo any compression or elongation, which is situated at a distance n from the bottom of the beam.[4,25,26] Meanwhile, the top and bottom surfaces receive the largest uniaxial compressive and tensile stresses, respectively. The compressive stress linearly decreases on penetrating into the beam in the x-axis direction, and finally becomes zero at the neutral surface, after which the tensile stress gradually increases at the lower part of the beam. Then the compressive strain $\hat{\varepsilon}$ at the top surface can be defined with respect to any small angle ϕ as follows:

$$\hat{\varepsilon} = \frac{(r-t)\phi - (r-n)\phi}{(r-n)\phi} = -\frac{(t-n)}{(r-n)} \quad (1)$$

According to the above equation, it is necessary to determine the position of the neutral surface n to calculate the applied strain. Assuming the beam material is Hookian, the neutral surface passes through a centroid of the cross-sectional area of the body.[4] For example, in the case of the line pattern shown in Fig. 1c, even if it has the same thickness t, the neutral plane can vary depending on the geometry of the cross section of the beam. In this case, the position of the neutral surface n_T is represented with respect to dimensionless geometric parameters as follows:

$$n_T = \frac{H}{2}\frac{1 + w'h'(h'+2)}{1 + w'h'} \quad (2)$$

where w' and h' are dimensionless parameters such that $w' = w/p$ and $h' = h/H$ (a more detailed derivation is provided in the ESI† with Fig. S2). In this way, when an elastomeric beam fabricated of PDMS is inserted into a recessed holder, lateral buckling is visually confirmed (Fig. 1d).

The morphology of lateral buckling differs depending on the degree of bending of the beam. For a quantitative study, the wavelength λ of the wrinkles is measured by varying the radius of the recessed holder r and the width of the wall w while maintaining $w' = 0.5$ for a constant n_T (Fig. 2a). To derive a scaling relationship, the actual system is regarded as the wall under compressive stress without bending. For further simplification, assume that the imposed compressive stress $\sigma(x) \sim \hat{\sigma} = \text{const}$, not a linear function of x. The width is much smaller than the length of the wall ($w \ll L$), hence bending occurs easier than compression at the wall. As a result, there is an out-of-plane deflection denoted as $\zeta(x,y)$ (Fig. 2b). The total energy of the system is composed of two parts: bending energy U_B which is predominant in the y-direction and deformation energy U_D in the presence of compression taking geometric constraint into account. The elastic bending energy due to deformation scales as $U_B \approx (B/2)\int_a (\zeta_{,yy})^2 \mathrm{d}a \sim BLhA^2/\lambda^4$ where B is the bending rigidity of the wall and A is the amplitude of wrinkles. (The notation $\zeta_{,yy}$ represents the second derivative of ζ with respect to y and da is a differential surface element of area in the xy plane.) Also, the deformation energy of the wall can be represented as $U_D \approx (\hat{\sigma}w/2)\int_a (\zeta_{,x})^2 \mathrm{d}a \sim \hat{\sigma}wLA^2/h$. A balance of these two energies gives the wavelength of the wrinkles as $\lambda \sim (B/\hat{\sigma}w)^{1/4}h^{1/2}$ which is consistent with the result of Cerda and Mahadevan.[27]

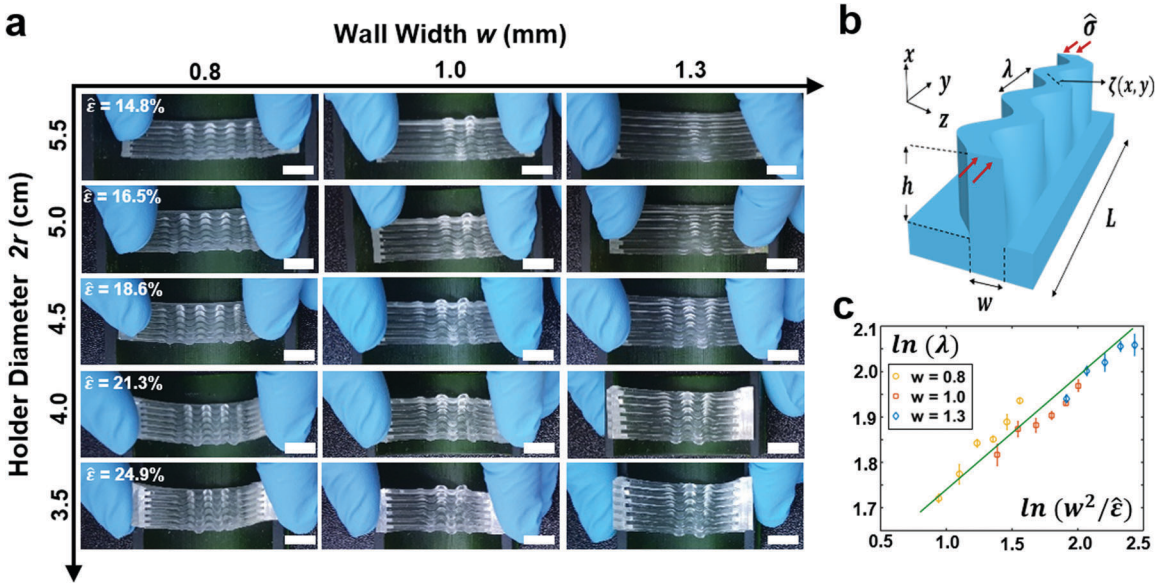

Fig. 2 (a) Images of lateral buckling varying with the radius of the holder r and the width of the wall w. Scale bars are 1 cm. Here, the compressive strain $\hat{\varepsilon}$ is represented in a positive sign for convenience. (b) Schematic illustration of the theoretical consideration of lateral buckling. (c) log–log plot of the wavelength λ varying with the wall width w and the strain $\hat{\varepsilon}$. Experimental data follow the scale with a slope of 0.25 as shown by the green line.

This indicates that the wavelength is chosen to be preferred from the competition of each energy. If the wall was not fixed to the substrate, it would have had one large deflection for compression. This is because the first mode of deformation is advantageous in terms of bending energy, whereas the deformation energy arising from the longitudinal inextensibility of the wall makes the buckling have a shorter wavelength.[22,27,28] This is analogous to the wrinkle formation mechanism in the bilayer system which compromises the intermediate wavelength between the stiffnesses of each layer such that $\lambda \sim (E_f/E_s)^{1/3}$, where E_f and E_s are Young's modulus of the thin film and the substrate, respectively.[18,27] Then, we rewrite the wavelength of our system as the relationship between the strain $\hat{\varepsilon}$ and width of the wall w to examine the experimental results. Since bending rigidity B and compressive stress $\hat{\sigma}$ scale as $B \sim Ew^3$ and $\hat{\sigma} \sim E\hat{\varepsilon}$, the wavelength λ is represented as follows:

$$\lambda \sim (w^2/\hat{\varepsilon})^{1/4} \quad (3)$$

To verify the above relationship, Fig. 2c shows the log–log plot of $(w^2/\hat{\varepsilon})$ *vs.* λ and experimental data are in good agreement with the theoretical line whose slope is 0.25. Through this relationship, it can be seen that the wavelength is shortened when the strain is applied more. Furthermore, applying the same strain, the smaller the width of the wall, the better the wrinkles are. In other words, lateral buckling can be formed well with the wall of a high aspect ratio. It should be noted that we multiplied a conversion factor considering the relationship between a chord and an arc because a wavy pattern forms along the contour of the recessed holder.

Using a 3D printer, however, it is difficult to fabricate high aspect ratio patterns due to the limitations of resolution. To overcome this problem, a ratchet structure whose cross section is shown in Fig. 3a was constructed. With these ratchet beams, the configuration of lateral buckling is investigated according to the strain change in the same manner as before. Unlike the line pattern, there is a large variance in the shape of the wrinkles at the edges due to the asymmetry, thus we only focused in the middle section of the beam (Fig. 3b). Considering the inextensibility, the amplitude of wrinkles in the ratchet beam is given as follows:[27]

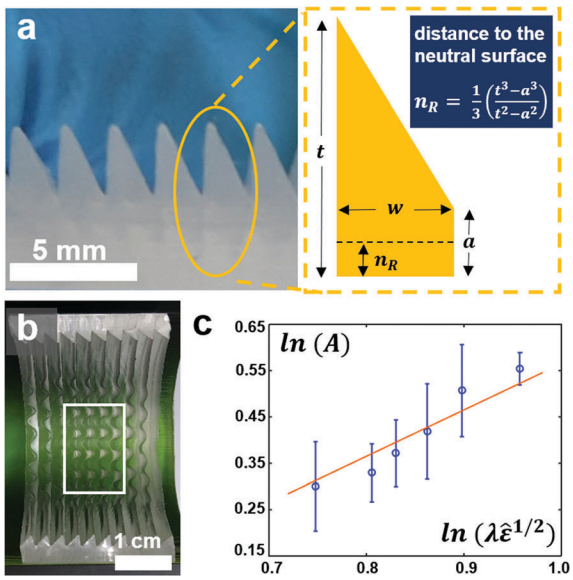

Fig. 3 (a) Cross-sectional image of the ratchet structure and definition of the distance to the neutral surface n_R (ESI,† Fig. S3). (b) Top view of the lateral buckling of the ratchet structure. For an accurate measurement, we focused on the wrinkles within the white boundary. (c) log–log plot of the amplitude of buckling A and the value of $\lambda\hat{\varepsilon}^{1/2}$ with a theoretical line whose slope is 1.0. The theoretical prediction of the linear dependence of the logarithmic value of amplitude of buckling A on that of $\lambda\hat{\varepsilon}^{1/2}$ shows an agreement with the experimental observation.

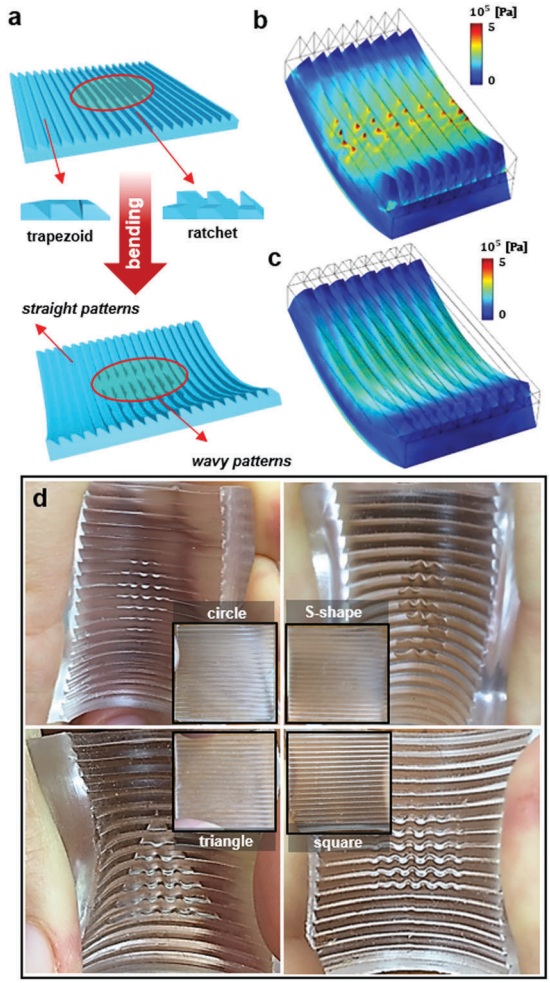

Fig. 4 (a) Schematic illustration of deformation differences for the same curvature in beams with a trapezoidal or ratchet structure. FE simulation results of stress distribution in (b) ratchets and (c) trapezoids of the beam under equal bending. The average undulation period in (b) is approximately 5 mm, which is similar to that of the experiments ($\lambda \sim 5.4$ mm). (d) Demonstration of the optical difference in ratchet and trapezoidal structures under bending. Insets show there is no difference in the patterns before bending.

$$A \sim \lambda \hat{\varepsilon}^{1/2} \quad (4)$$

The experimental results confirmed the above equation as shown in Fig. 3c.

By removing the upper parts from the ratchet structure, a beam having both ratchets and trapezoids can be obtained. If it is bent, lateral buckling occurs in the part of the ratchets only, but not in the one of the trapezoids, so it can be expected to have an optical difference at the same curvature (Fig. 4a).

It can be qualitatively said that in the trapezoidal structure not only is the strain reduced using eqn (1) due to a decrease in the thickness t, but also the width w is relatively increased. To understand this behaviour more precisely, finite element (FE) simulations were carried out.[29] In Fig. 4b and c, undulation occurs due to stress concentration at the tip of the ratchet structure, whereas there is no deformation in the trapezoidal one. When there is no bending, looking down at the beam from the top shows no difference between both structures. By applying the curvature, however, wrinkles only occur in a portion having a ratchet structure, which causes a visual difference. By using this, various shapes or characters can be quite freely generated and disappeared according to the bending and releasing of the beam (Fig. 4d). We note that the sizes of the figures or letters can be reduced by using conventional semiconductor processing such as photolithography followed by dry etching to realize high aspect ratio wall patterns. The conceptual demonstration of lateral buckling of the desired area can be exploited to anti-counterfeit patterns, which can be seen when we bend flexible films. Also, strain sensors can be another application, in which patterns can be generated when the strain is greater than a critical value.

In summary, we present the lateral buckling of elastomeric line patterns with various structures fabricated with soft lithography. We demonstrate that the shape of the wrinkles depends on the curvature and geometry of the beam based on the scaling concepts and also control it. Furthermore, we can create some mechano-responsive patterns at a selected area by designing the structure of the beam. Soft matter with the advantages of lightness, deformability and biocompatibility is known to have the potential to be used in diverse applications when it has tunable pattern formation. Therefore, this study may not only account for the mechanical instability of lateral buckling, but also provide a strategy for manufacturing high-technology devices.

Conflicts of interest

There are no conflicts to declare.

Acknowledgements

H. Lee and J. G. Bae contributed equally to this work. This work was supported by the National Research Foundation of Korea (NRF) grant funded by the Korean government (MSIP) (2016R1A2B4013640 and 2015R1A2A2A01007379) and Samsung Display.

Notes and references

1 S. P. Timoshenko and J. M. Gere, *Theory of elastic stability*, 1961.
2 G. A. Howard, *Analysis and design of structural sandwich panels*, Oxford, Pergamon Press, 1969.
3 J. W. Clark and H. N. Hill, *J. Struct. Div.*, 1960, **86**, 175–196.
4 J. Gere and B. Goodno, *Mechanics of materials*, Nelson Education, 2012.
5 J. W. Hutchinson, M. D. Thouless and E. G. Liniger, *Acta Metall. Mater.*, 1992, **40**, 295–308.
6 N. Bowden, S. Brittain, A. G. Evans, J. W. Hutchinson and G. M. Whitesides, *Nature*, 1998, **393**, 146–149.
7 K. Dalnoki-Veress, B. G. Nickel and J. R. Dutcher, *Phys. Rev. Lett.*, 1999, **82**, 1486–1489.
8 W. T. S. Huck, N. Bowden, P. Onck, T. Pardoen, J. W. Hutchinson and G. M. Whitesides, *Langmuir*, 2000, **16**, 3497–3501.

9 C. M. Stafford, C. Harrison, K. L. Beers, A. Karim, E. J. Amis, M. R. VanLandingham, H.-C. Kim, W. Volksen, R. D. Miller and E. E. Simonyi, *Nat. Mater.*, 2004, **3**, 545–550.
10 E. P. Chan, E. J. Smith, R. C. Hayward and A. J. Crosby, *Adv. Mater.*, 2008, **20**, 711–716.
11 S. H. Chae, W. J. Yu, J. J. Bae, D. L. Duong, D. Perello, H. Y. Jeong, Q. H. Ta, T. H. Ly, Q. A. Vu, M. Yun, X. Duan and Y. H. Lee, *Nat. Mater.*, 2013, **12**, 403–409.
12 P. Kang, M. C. Wang, P. M. Knapp and S. W. Nam, *Adv. Mater.*, 2016, **28**, 4565.
13 P. J. Yoo, K. Y. Suh, S. Y. Park and H. H. Lee, *Adv. Mater.*, 2002, **14**, 1383–1387.
14 K. Efimenko, M. Rackaitis, E. Manias, A. Vaziri, L. Mahadevan and J. Genzer, *Nat. Mater.*, 2005, **4**, 293–297.
15 S. J. Kwon and H. H. Lee, *J. Appl. Phys.*, 2005, **98**, 63526.
16 M. Guvendiren, J. A. Burdick and S. Yang, *Soft Matter*, 2010, **6**, 2044.
17 D. Chandra and A. J. Crosby, *Adv. Mater.*, 2011, **23**, 3441–3445.
18 J. Groenewold, *Physica A*, 2001, **298**, 32–45.
19 X. Chen and J. W. Hutchinson, *J. Appl. Mech.*, 2004, **71**, 597.
20 B. Audoly and A. Boudaoud, *J. Mech. Phys. Solids*, 2008, **56**, 2401–2421.
21 J. Song, H. Jiang, Z. J. Liu, D. Y. Khang, Y. Huang, J. A. Rogers, C. Lu and C. G. Koh, *Int. J. Solids Struct.*, 2008, **45**, 3107–3121.
22 H. Yoon, A. Ghosh, J. Y. Han, S. H. Sung, W. B. Lee and K. Char, *Adv. Funct. Mater.*, 2012, **22**, 3723–3728.
23 J. Li, Y. Cho, I. S. Choi and S. Yang, *Adv. Funct. Mater.*, 2014, **24**, 2361–2366.
24 C. Lestringant, C. Maurini, A. Lazarus and B. Audoly, *Phys. Rev. Lett.*, 2017, **118**, 165501.
25 C. L. Dym and I. H. Shames, *Solid mechanics: A variational approach, augmented edition*, 2013.
26 L. D. Landau, A. M. Kosevich, L. P. Pitaevskii and E. M. Lifshitz, *Theory of elasticity*, 1986.
27 E. Cerda and L. Mahadevan, *Phys. Rev. Lett.*, 2003, **90**, 74302.
28 Y. Ebata and A. J. Crosby, *Soft Matter*, 2014, **10**, 1963–1968.
29 G. A. Holzapfel, *Nonlinear Solid Mechanics: A Continuum Approach for Engineering*, 2000.